Activity measurements of the radionuclides ^{18}F, ^{64}Cu and ^{99m}Tc for the ANSTO, Australia, in the ongoing comparisons BIPM.RI(II)-K4 series and KCRV update in the corresponding BIPM.RI(II)-K1 comparison

C. Michotte[1], M. Nonis[1], W.M. Van Wyngaardt[2], S. Tobin[2], M. Smith[2], S. Lee[2], T. Jackson[2], J. Ilter[2], B. Howe[2], A. Sarbutt[2] and I. Da Silva[3]

[1] Bureau International des Poids et Mesures (BIPM), 92 310 Sèvres
[2] Australian Nuclear Science and Technology Organisation (ANSTO), Lucas Heights, Australia
[3] CNRS/CEMHTI, Orléans, France

Abstract

In 2017, comparisons of activity measurements of ^{18}F, ^{64}Cu and ^{99m}Tc using the Transfer Instrument of the International Reference System (SIRTI) took place at the Australian Nuclear Science and Technology Organisation (ANSTO, Australia). Ampoules containing ^{18}F, ^{64}Cu and ^{99m}Tc solutions were measured in the SIRTI for about 1.7 to 4 half-lives. The ANSTO carried out the primary standardization of the activity in the ampoules by $4\pi(LS)\beta-\gamma$ coincidence measurements. The comparisons, identifiers BIPM.RI(II)-K4.F-18, BIPM.RI(II)-K4.Cu-64 and BIPM.RI(II)-K4.Tc-99m are linked to the corresponding BIPM.RI(II)-K1.F-18, BIPM.RI(II)-K1.Cu-64 and BIPM.RI(II)-K1.Tc-99m comparisons. The BIPM.RI(II)-K1 ^{18}F and ^{99m}Tc key comparison reference values have been updated to include the latest BIPM.RI(II)-K4 linked results and degrees of equivalence for those three comparisons have been evaluated.

1. Introduction

Radionuclides with half life often much less than a day are essential for nuclear medicine and particularly for medical imaging. The use of nuclear medicine is increasing with the accessibility of these radionuclides which are consequently of great interest to the National Metrology Institutes (NMIs) in terms of standardization and SI traceability. However, sending ampoules of short-lived radioactive material to the Bureau International des Poids et Mesures (BIPM) for measurement in the International Reference System (SIR) [1] is only practicable for the NMIs that are based in Europe and near to the BIPM. Consequently, to extend the utility of the SIR and enable other NMIs to participate, a transfer instrument (SIRTI) has been developed at the BIPM with the support of the Consultative Committee for Ionizing Radiation CCRI(II) Transfer Instrument Working Group [2].

The BIPM ongoing K4 comparisons of activity measurements of ^{18}F (half life $T_{1/2}$ = 1.8288(3) h [3])[1], ^{64}Cu ($T_{1/2}$ = 12.7004(20) h [4]) and ^{99m}Tc ($T_{1/2}$ = 6.0067(10) h [3]) are based on the SIRTI, a well-type NaI(Tl) crystal calibrated against the SIR, which is moved to each participating laboratory. The stability of the system is monitored using a ^{94}Nb reference source (half life of 20 300(1 600) years [5]) from the Joint Research Centre of the European Commission (JRC, Geel), which also contains the ^{93m}Nb isotope. The ^{18}F, ^{64}Cu or ^{99m}Tc count rate above a low-energy threshold, defined by the ^{93m}Nb x-ray peak at 16.6 keV, is measured relative to the ^{94}Nb count rate above the same threshold. Once the threshold is set, a brass liner is placed in the well to suppress the ^{93m}Nb contribution to the ^{94}Nb stability measurements. It should be noted that the uncertainty associated with the ^{94}Nb decay correction is negligible. The ^{99m}Tc SIR ampoule is placed in the detector well in a brass liner; for the ^{18}F and ^{64}Cu SIR ampoules, a PVC (polyvinyl chloride) liner is used instead to stop the β^+ particles while minimizing the production of bremsstrahlung. No extrapolation to zero energy is carried out as all the measurements are made with the same threshold setting. The live-time technique using the MTR2 module from the Laboratoire National d'Essais – Laboratoire National Henri Becquerel, France (LNE-LNHB) [6] is used to correct for dead-time losses, taking into account the width of the oscillator pulses. The standard uncertainty associated with the live-time correction, due to the effect of the finite frequency of the oscillator, is negligible.

Similarly to the SIR, a SIRTI equivalent activity, A_E, is deduced from the ^{18}F, ^{64}Cu or ^{99m}Tc and the ^{94}Nb counting results and the ^{18}F, ^{64}Cu or ^{99m}Tc activity measured by the NMI. A_E is inversely proportional to the detection efficiency, i.e. A_E is the activity of the source measured by the participant divided by the ^{18}F, ^{64}Cu or ^{99m}Tc count rate in the SIRTI relative to the ^{94}Nb count rate. The possible presence of impurity in the solution should be accounted for using γ-ray spectrometry measurements carried out by the NMI.

The present ^{18}F, ^{64}Cu and ^{99m}Tc K4 comparisons are linked to the corresponding BIPM.RI(II)-K1 comparisons through the calibration of the SIRTI against the SIR at the BIPM and, consequently, the degrees of equivalence with the K1 key comparison reference value (KCRV) can be evaluated. The K4 ^{18}F and ^{99m}Tc comparison results based on primary measurements carried out by the NMI, or ionization chamber measurements traceable to primary ^{18}F and ^{99m}Tc measurements are eligible for inclusion in the KCRV, with some restrictions.

The protocol [7] and previous comparison results for the BIPM.RI(II)-K4 comparisons are available in the key comparison database of the CIPM (International Committee on Weights and Measures) Mutual Recognition Arrangement [8]. Publications concerning the details of the SIRTI and its calibration against the SIR can be found elsewhere [9, 10].

2. Participants

As detailed in the protocol, participation in the BIPM.RI(II)-K4 comparisons mainly concerns member states that are located geographically far from the BIPM (except for ^{11}C) and that have developed a primary measurement method for the radionuclide of concern. However, at the time of the comparison, the NMI may decide for convenience to use a secondary method, for example a calibrated ionization chamber. In this case, the traceability of the calibration needs to be clearly identified.

[1] Hereafter, the last digits of the standard uncertainties are given in parenthesis.

The present comparisons took place at the Australian Nuclear Science and Technology Organisation (ANSTO), Lucas Heights, Australia, in November 2017, who used for the activity standardizations an ionization chamber (IC) calibrated by 4π(LS)β–γ coincidence.

3. The SIRTI at the ANSTO

The reproducibility and stability of the SIRTI at the ANSTO were checked by measuring the count rate produced by the reference ^{94}Nb source No. 1, the threshold position (defined by the ^{93m}Nb x-ray peak), the background count rate, the frequency of the oscillator No. 1 for the live-time correction and the room temperature as shown in Figure 1a. The plots shown in the Figure represent the differences from the values indicated in the figure caption, using the appropriate units, as given, for each quantity measured.

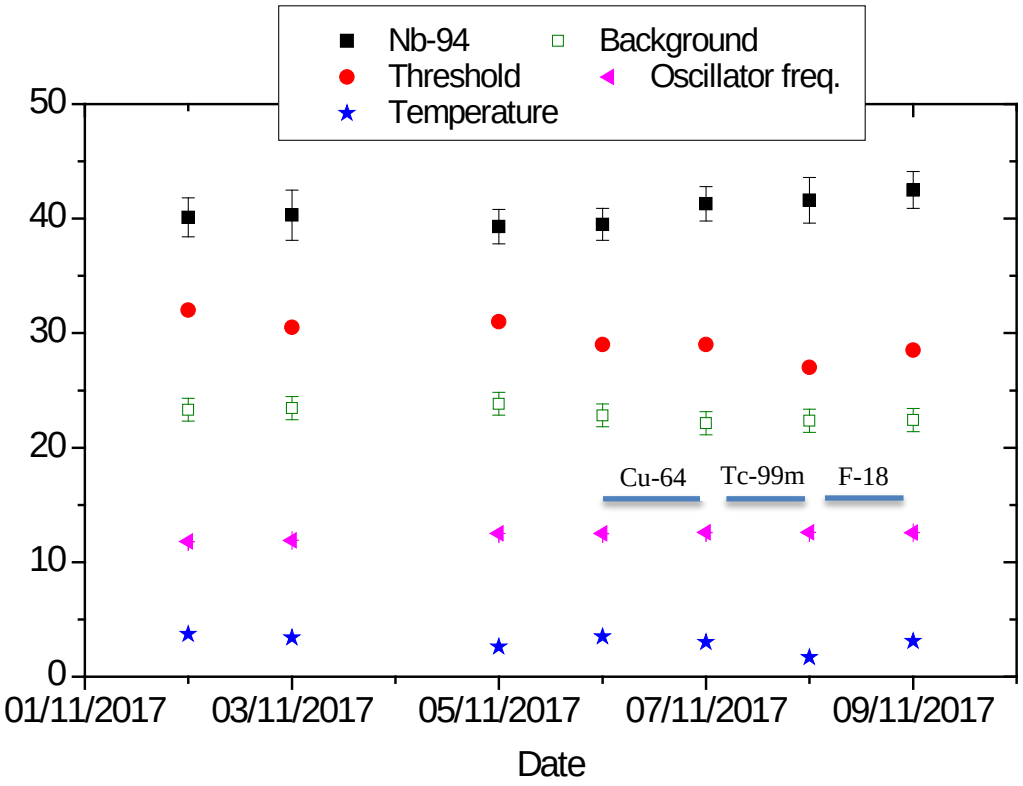

Figure 1a: Fluctuation of the SIRTI at the ANSTO. Filled squares: ^{94}Nb source No.1 count rate / s^{-1} above 8450 s^{-1}; triangles: frequency of the oscillator No.1 / Hz above 999 990 Hz; circles: threshold position / channel above 70 channels; asterisks: room temperature / °C above 20 °C; open squares: background count rate / s^{-1} above 55 s^{-1}. Statistical uncertainty (k = 1) for the Nb count rate, background count rate and oscillator frequency are shown (in some cases, the uncertainties are not visible in the plot as they are hidden by the character printed for the data point).

The SIRTI background measured at the ANSTO suffered small interferences from other radioactive sources used nearby (see Figure 1b). Consequently, a type B uncertainty of 1 s^{-1} has been added quadratically to all the background rate uncertainties in the comparison.

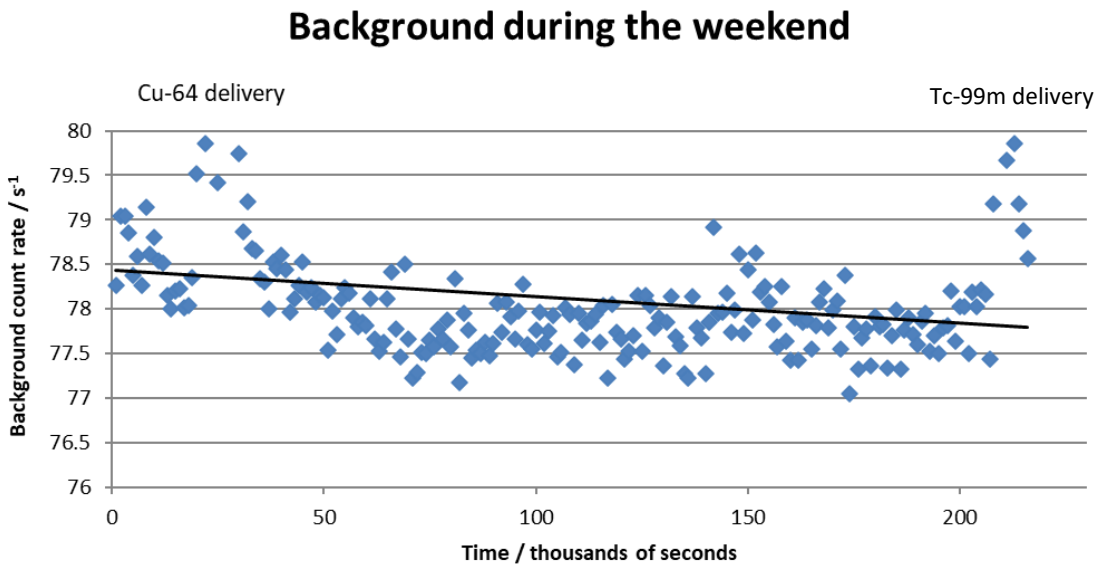

Figure 1b: Example of background rate fluctuations when sources were used in the vicinity of the SIRTI. When strong ^{226}Ra sources were used in the ANSTO ionization chamber, increase of the SIRTI background rate by 1 s^{-1} was also observed. The black line is to guide the eye.

The temperature in the laboratory and the SIRTI oscillator frequency were very stable. Nevertheless, the ^{94}Nb measurement results show a slow increasing trend (~3 x 10^{-4} change in relative count rate in 7 days) while the threshold position is decreasing. However, as the comparison result is proportional to a ratio of the radionuclide compared and the ^{94}Nb reference source count rates, these slow fluctuations should not impact the comparison results. In addition, all the ^{94}Nb count rates agree within standard uncertainty giving a reduced chi-squared value of 0.56.

The weighted mean of the ^{94}Nb source No. 1 count rates measured at the ANSTO, corrected for live-time, background, and decay, was 8490.54(62) s^{-1} and was used to normalize all the comparison measurement data. This mean value differs by 2 parts in 10^4 with the weighted mean of the ^{94}Nb source No. 1 count rate since the set-up of the system in March 2007, 8492.56(19) s^{-1} and this was taken into account in the uncertainty budget. Finally, on the return of the SIRTI to the BIPM after the ANSTO comparison, the ^{94}Nb count rate was checked giving a value of 8489.9(13) s^{-1} in agreement with the measurements carried out at the ANSTO.

4. The ^{18}F, ^{64}Cu and ^{99m}Tc solutions standardized at the ANSTO

The ^{18}F, ^{64}Cu and ^{99m}Tc solutions measured in the SIRTI are described in Table 1, including any impurities, when present, as identified by the laboratory.

The density and volume of the solutions in the ampoules conformed to the K4 protocol requirements. All ampoules were centrifuged and no drops were observed on their walls.

Table 1: Characteristics of the solutions measured in the SIRTI

Radionuclide	**Solvent / mol dm^{-3}**	**Carrier / μg g^{-1}**	**Density at 20 °C / g cm^{-3}**	**Ampoule number**	**Mass / g**	**Impurity***
^{18}F (FDG)	water	-	1.000(2)	F18-1867-D1-A3	3.6061(1)	None detected
				F18-1867-D1-A4	3.5802(1)	
^{64}Cu	HCl / 0.1	Cu^{2+} / 16.6	1.003(5)	Cu64-1867-M1-A2	3.5512(1)	None detected
				Cu64-1867-M1-A3	3.6395(1)	
				Cu64-1867-M1-A4	3.5653(1)	
^{99m}Tc	water	NaCl / 45	1.000(2)	Tc99m-1867-M1-A2	3.6207(1)	None detected
		NaCl / 41	1.000(2)	Tc99m-1867-D1-A4	3.5900(1)	

* Ratio of the impurity activity to the main radionuclide activity at the reference date

The ANSTO activity measurement results are summarized in Table 2. The uncertainty budgets are given in Table 3.

Table 2: The ^{18}F, ^{64}Cu and ^{99m}Tc standardizations by the ANSTO

Radionuclide	**Measurement method** ACRONYM*	**Activity conc. / kBq g^{-1}**	**Reference date** YYYY-MM-DD	**Half life used by the NMI / h**
^{18}F	Ionization Chamber calibrated in June 2017 by 4π(LS)β$^+$-(NaI)γ coincidence 4P-IC-GR-00-00-00 4P-LS-PO-NA-GR-CO	Ampoule D1-A3: 7.124(29) Ampoule D1-A4: 5.705(23)	2017-11-08 3:00 UTC	1.828 90(23)
^{64}Cu	Ionization Chamber calibrated in February 2018 by 4π(LS)β-(NaI)γ coincidence 4P-IC-GR-00-00-00 4P-LS-MX-NA-GR-CO	Ampoule M1-A2: 30.27(43) Ampoule M1-A3: 28.11(40) Ampoule M1-A4: 30.85(44)	2017-11-06 1:00 UTC	12.7004(20)
^{99m}Tc	Ionization Chamber calibrated in October 2018 by 4π(LS)ce-(NaI)γ coincidence 4P-IC-GR-00-00-00 4P-LS-CE-NA-GR-CO	Ampoule M1-A2: 8.651(77) Ampoule D1-A4: 7.802(69)	2017-11-07 3:00 UTC	6.0067(10)

* See appendix 1

Table 3: The ANSTO uncertainty budgets for the activity standardizations of the ^{99m}Tc, ^{18}F and ^{64}Cu ampoules

Uncertainty contributions due to	**Evaluation method**	**Relative standard uncertainty × 10^4 and comments**					
		^{18}F		**^{64}Cu**		**^{99m}Tc**	
Counting statistics	A	1	Standard deviation of the mean for 250x10 current measurements	1	Standard deviation of the mean for 50x100 current measurements	1	Standard deviation of the mean for 500x10 current measurements
Weighing	B	6	Weighing and solution handling	4	Weighing and solution handling	7	Weighing and solution handling
Background	A	1	Statistical variation in background	1	Statistical variation in background	1	Statistical variation in background
Impurities	B	–	None detected by gamma spectroscopy	–	None detected by gamma spectroscopy or ionization chamber measurement for > 5 half-lives of Cu-64	–	None detected by gamma spectroscopy or ionization chamber measurement for > 3.6 half-lives of Tc-99m
Half life	B	0.4	Maximum decay correction from IC measurement to SIRTI reference date	5.7	Maximum decay correction from IC measurement to SIRTI reference date	3.8	Maximum decay correction from IC measurement to SIRTI reference date
IC calibration factor	B	38	Primary standardization and calibration of IC	140	Primary standardization and calibration of IC	87	Primary standardization and calibration of IC
Non-linearity	B	10	Non-linearity of IC response between current range for calibration and for SIRTI measurements	10	Non-linearity of IC response between current range for calibration and for SIRTI measurements	–	
Geometry effect	B	–		–		10	Previously determined, variation due to glass thickness and source positioning in IC
Relative combined standard uncertainty		**40**		**141**		**88**	

4.1 *^{18}F ANSTO measurement details*

The inter-comparison master solution was standardized by measuring an ampoule containing 3.5645 g of this solution in the calibrated ionization chamber. A dilution of the master solution was prepared (dilution factor = 29.700(5)) and the dilution factor confirmed by measuring an ampoule containing 3.5900 g of the dilution in the calibrated ionization chamber. The ampoules F18-1867-D1-A3 and F18-1867-D1-A4 were prepared by pycnometer dispensing of 0.11268 g and 0.08959 g, respectively, of the dilution and filled to a total mass of 3.6061 g and 3.5802 g, respectively, using deionized water. The activity of sources F18-1867-D1-A3 and F18-1867-D1-A4 were calculated from the dispensed mass, the dilution factor and the activity concentration of the master solution.

The ionization chamber (IC) was calibrated in June 2017 at ANSTO by the $4\pi(LS)\beta^+$-(NaI)γ coincidence extrapolation method. One source from the master solution and one source from a dilution (DF = 67.77 (3)) were counted for five repeats of 100 seconds real time at each of 11 LS efficiency points. LS discrimination levels were adjusted manually, with the lowest LS threshold excluding all emissions associated with the electron capture decay branch. A gamma window was set over the 511 keV annihilation γ-ray full-energy peak. Two results were obtained for each source, applying either the logical sum of the double coincidences, or the triple coincidences, for the LS channel. Linear extrapolation and a correction for the β^+/EC branching ratio = 0.9686 (19) provided the source activity. The final result was calculated as the weighted mean of four results, taking the dilution factor into account. LS source measurements extended over > 12 half-lives of ^{18}F. A detailed uncertainty budget for the IC's calibration is given in Appendix 2a.

4.2 *^{64}Cu ANSTO measurement details*

The inter-comparison master solution was standardized by measuring an ampoule containing 3.5968 g of this solution in the calibrated ionization chamber. The ampoules Cu-64-1867-M1-A2, Cu-64-1867-M1-A3 and Cu-64-1867-M1-A4 were prepared by pycnometer dispensing of 0.25367 g, 0.24141 g and 0.25956 g, respectively, of the master solution and filled to a total mass of 3.5512 g, 3.6395 g and 3.5653 g, respectively, using carrier solution. The activity of sources Cu-64-1867-M1-A2, Cu-64-1867-M1-A3 and Cu-64-1867-M1-A4 were calculated from the dispensed mass and the activity concentration of the master solution.

The IC was calibrated in February 2018 at ANSTO by the $4\pi(LS)e_{A,X}$-(NaI)γ coincidence extrapolation method. One source from the master solution and two sources from a dilution (DF = 8.280 (4)) were each counted for at least 10 repeats of 350 seconds real time at each of 11 LS efficiency points. LS discrimination levels were adjusted manually. A gamma window was set over the 1345.7 keV γ-ray full energy peak (intensity 0.47 %). Measurements were complicated by background counts from the ^{40}K 1460.822 keV γ-ray peak, contributing 0.52 % to the overall uncertainty. Data was plotted as BG/C vs (N_C/N_G-1) and fitted to 1st order polynomials using orthogonal distance regression, which takes into account uncertainties on the X- and Y-axes. Uncertainties applied were the observed statistical uncertainties. The intercept was multiplied by a correction F = 0.9980 (21), to account for the different detection probabilities for the $ec_{0,0}$ and $ec_{1,0}$ branching ratios [33]. A detailed uncertainty budget for the IC's calibration is given in Appendix 2b.

4.3 *^{99m}Tc ANSTO measurement details*

The inter-comparison master solution was standardized by measuring an ampoule containing 3.6686 g of this solution in the calibrated ionization chamber. The ampoule Tc99m-1867-M1-A2 was prepared by pycnometer dispensing of 0.01817 g of the master solution and filled to a total mass of 3.6207g using deionized water. A dilution of the master solution was prepared (dilution factor = 13.008(2)) and an ampoule containing 3.5987 g of the dilution measured in the ionization chamber as a cross-check. The ampoule Tc-99m-1867-D1-A4 was prepared by pycnometer dispensing of 0.21129 g of the dilution and filled to a total mass of 3.5900 g using deionized water. The activity of sources Tc99m-1867-M1-A2 and Tc-99m-1867-D1-A4 were calculated from the dispensed mass, the activity concentration of the master solution and the dilution factor where relevant.

The IC was calibrated in October 2018 at ANSTO by 4π(LS)ce-(NaI)γ coincidence extrapolation method (see [34] for details on the standardisation). A detailed uncertainty budget for the IC's calibration is given in Appendix 2c.

5. The ^{18}F, ^{64}Cu and ^{99m}Tc measurements in the SIRTI at the ANSTO

The maximum live-time corrected count rate in the NaI(Tl) was 18 000 s^{-1} for ^{18}F, 16 500 s^{-1} for ^{64}Cu and, 19 000 s^{-1} for ^{99m}Tc, which conform to the limit of 20 000 s^{-1} set in the protocol [7]. In addition, a relative standard uncertainty of 2×10^{-4}, 3×10^{-4} and 4×10^{-4} for ^{18}F, ^{64}Cu and ^{99m}Tc respectively, was added to take account of a possible drift in the SIRTI at high count rate [9]. The time of each SIRTI measurement was obtained from the synchronization of the SIRTI laptop with the ANSTO NTP time server.

In principle, the live-time correction should be modified to take into account the decaying count rate [11]. In the present experiments, the duration of the measurements made at high rate has been limited to 400 s, 700 s and 500 s for ^{18}F, ^{64}Cu and ^{99m}Tc, respectively, so that the relative effect of decay on the live-time correction is less than one part in 10^4.

Two ampoules of ^{18}F and ^{99m}Tc solutions were measured alternatively for about 4 and 3 half-lives, respectively. Three ampoules of ^{64}Cu were measured alternatively for about 1.7 half-lives. The results are shown in Figures 2a-2c.

For ^{18}F (see Figure 2a), ampoule D1-A3 looks lower than ampoule D1-A4 however, the difference is not significant at $k = 2$. Both ampoules were used in the data analysis, giving a reduced chi-squared value $\chi^2 = 1.7$.

For ^{64}Cu, the SIRTI results in Figure 2b show a significant difference of 0.14 % between the ampoules M1-A2 and M1-A4. A third ampoule from the same mother solution (M1-A3) was measured giving a mean result in agreement with ampoule M1-A4. No reason could be identified for the discrepancy of ampoule M1-A2: the ampoule glass wall effect for γ-ray energies above 500 keV (evaluated by Monte-Carlo simulations) should not be larger than 5 parts in 10 000; the ampoules were centrifuged and no drops were observed; the IC measurement results of these ampoules were consistent with a standard deviation of the activity concentration of the master solution determined from the three ampoule measurements of 0.0054 %. Consequently, it was decided to analyze the data from the three ampoules all together

(χ^2 = 2.0), giving a SIRTI equivalent activity of A_E = 54.79(77) kBq, where a relative standard uncertainty component of 7×10^{-4} was added quadratically to take account of the discrepancy for ampoule M1-A2. It is worth noting that if ampoule M1-A2 is excluded from the analysis, χ^2 decreases to 0.70 but the comparison result, 54.78(77) kBq, remains almost unchanged. This happens because there are many more data points for ampoules M1-A3 and M1-A4 than for ampoule M1-A2.

For ^{99m}Tc, the reduced chi-squared value χ^2 is equal to 0.86. See Figure 2c.

The absence of significant trend in all three data sets confirms the stability and adequate live-time corrections of the SIRTI as well as the absence of significant impurity in the solutions.

The uncertainty budgets for the SIRTI measurements of the ^{18}F, ^{64}Cu and ^{99m}Tc ampoules are given in Table 4. In the SIRTI, the dominant part of the ^{64}Cu detection efficiency is defined by its beta plus decay. In this sense it is similar to ^{18}F, and the Monte-Carlo simulations carried out for ^{18}F were also used for the ^{64}Cu uncertainty evaluation. Further details are given in reference [9].

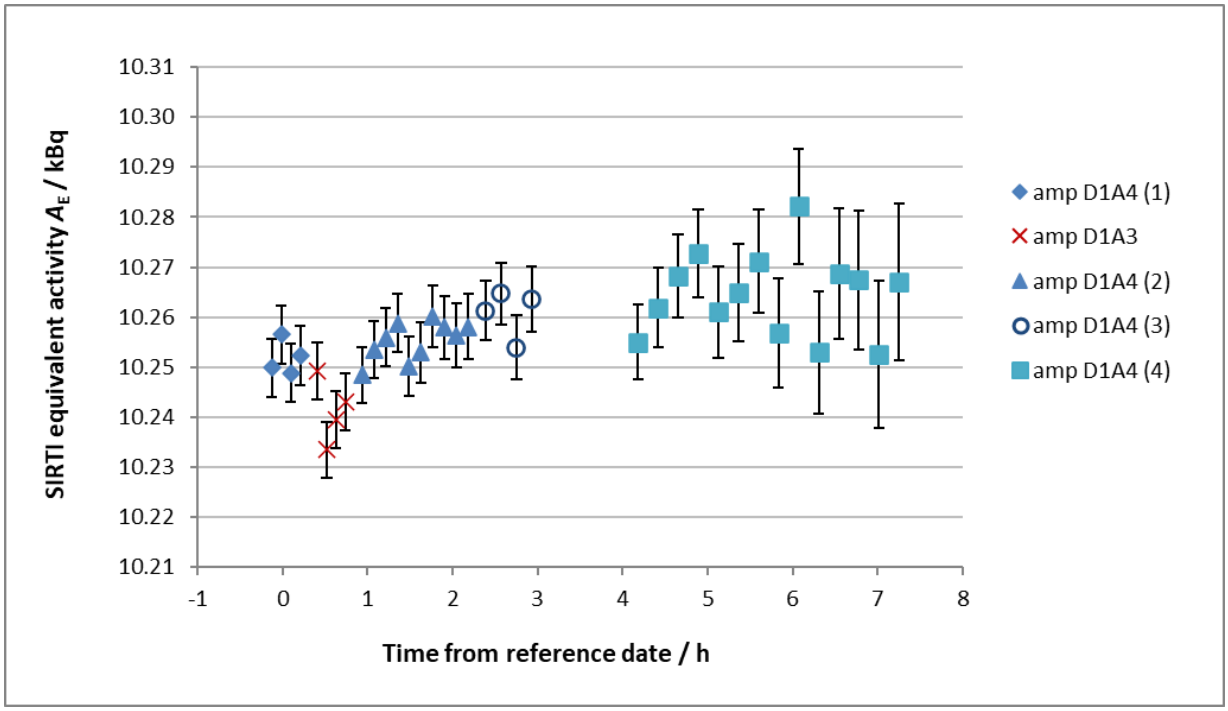

Figure 2a: ^{18}F measurement results in the SIRTI at the ANSTO. The uncertainty of the ^{18}F activity concentration, which is constant over all the measurements, is not included in the uncertainty bars shown on the graph.

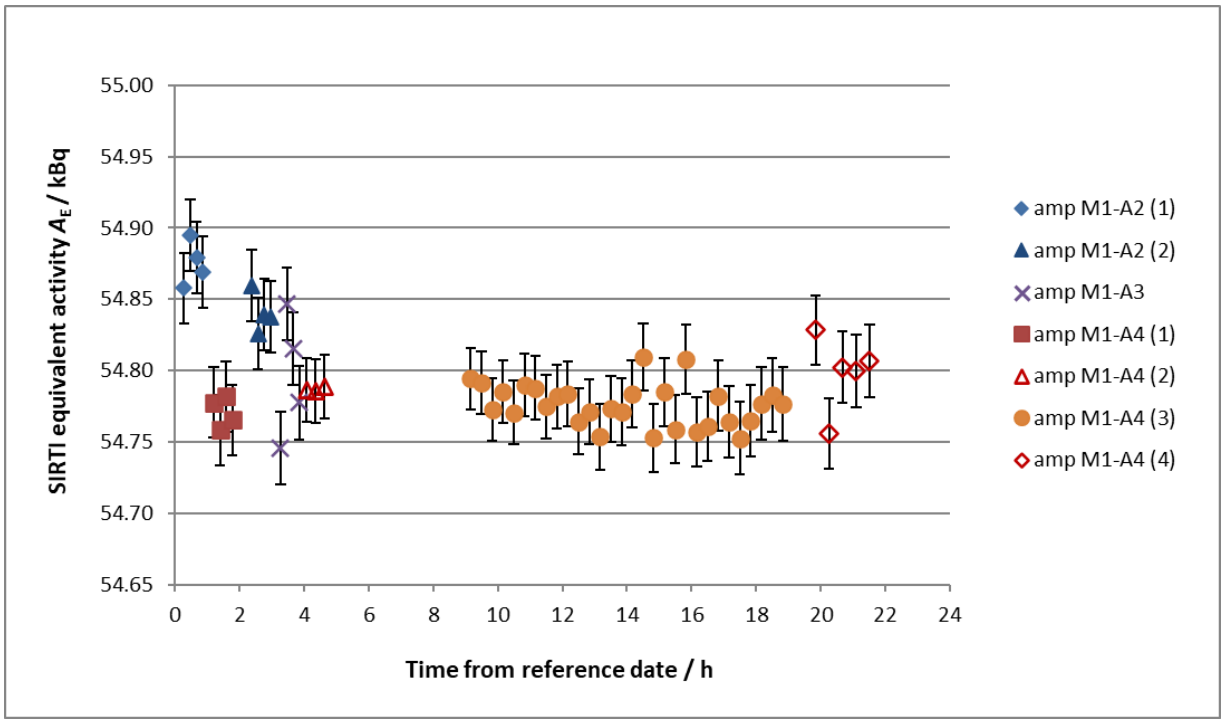

Figure 2b: As for Figure 2a, but for ^{64}Cu

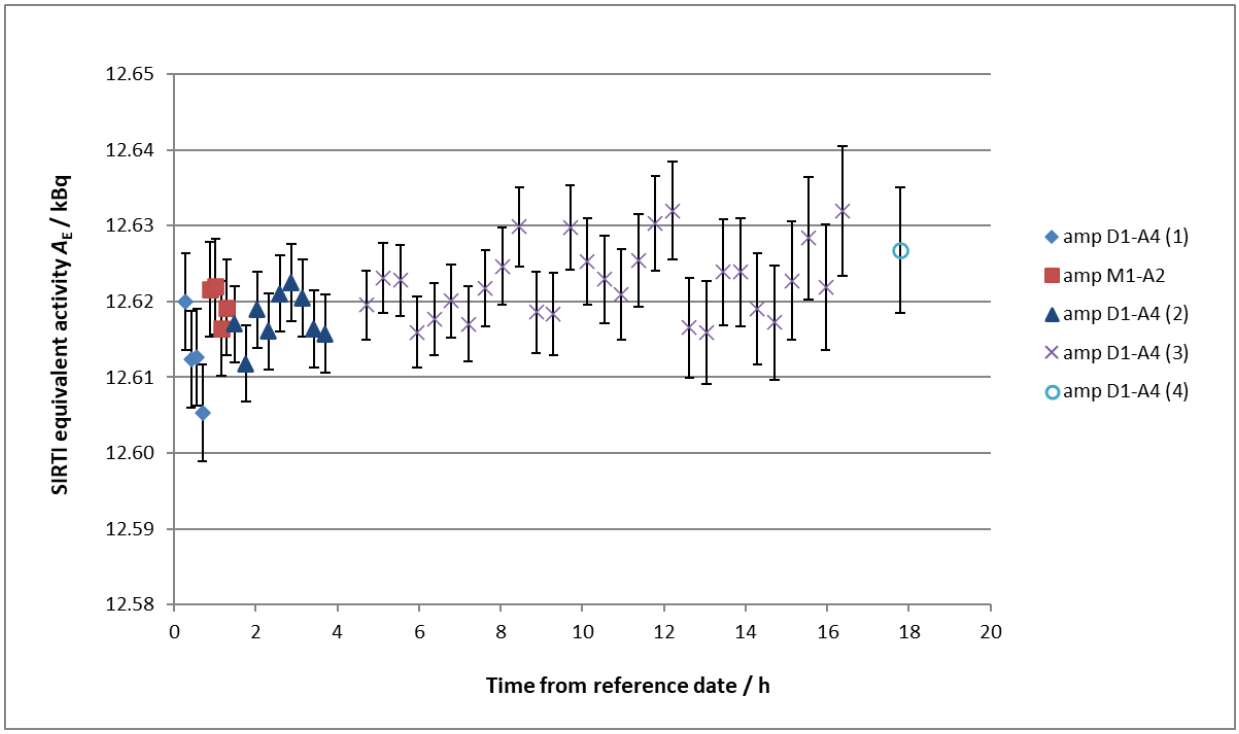

Figure 2c: As for Figure 2a, but for ^{99m}Tc.

Table 4: Uncertainty budgets for the SIRTI measurement of the ^{18}F, ^{64}Cu and ^{99m}Tc ampoules

Uncertainty contributions due to	**Comments**	**Evaluation method**	**Relative standard uncertainty × 10^4**		
			^{18}F	**^{64}Cu**	**^{99m}Tc**
Radionuclide count rate	Including live-time, background, decay correction and threshold setting	A	2.3§	1.5§§	2.3§§§
	From discrepancy observed between ampoules	B		7.1	
^{94}Nb count rate	Including live-time, background and threshold setting	A	0.7*	0.7*	0.7*
	From difference observed between mean ^{94}Nb rate at ANSTO and the mean value since 2007	B	2.4	2.4	2.4
Long-term stability of the SIRTI	Weighted standard deviation of 118 series of 10 measurements	A	0.2	0.2	0.2
Effect of decay on the live-time correction	Maximum measurement duration evaluated from [12]	B	< 1	< 1	< 1
SIRTI drift at high count rate	Mean possible drift over the radionuclide series of measurements at the ANSTO	B	2	3	4
Ampoule dimensions	From the JRC report [13] and sensitivity coefficients from Monte-Carlo simulations	B	2.2**	2.2**	8.4
Ampoule filling height	Solution volume is 3.6(1) cm^3; sensitivity coefficients from Monte-Carlo simulations	B	2.3	2.3**	2.8
Solution density	Between 1 g/cm^3 and 1.01 g/cm^3 as requested in the protocol; sensitivity coefficients from Monte-Carlo simulations	B	0.7	0.7	0.8
Drops on the ampoule walls	Ampoules centrifuged	B	–	–	–
Relative combined standard uncertainty			4.7	8.3	10

§ Standard uncertainty of the weighted mean of 36 measurements of 2 ampoules, taking into account correlation due to the ^{18}F half life
§§ Standard uncertainty of the weighted mean of 54 measurements of 3 ampoules, taking into account correlation due to the ^{64}Cu half life
§§§ Standard uncertainty of the weighted mean of 42 measurements of 2 ampoules, taking into account correlation due to the ^{99m}Tc half life
* Standard uncertainty of the weighted mean of 7 series of 10 measurements over 7 days
****** included in the uncertainty of the radionuclide count rate

6. Comparison results

The weighted mean and uncertainty of a selection of the measured A_E values is calculated taking into account correlations. The standard uncertainty $u(A_E)$ is obtained by adding in quadrature the SIRTI combined uncertainty from Table 4 and the uncertainty stated by the participant for the ^{18}F, ^{64}Cu and ^{99m}Tc measurements (see Table 3). The correlation between the ANSTO and the BIPM due to the use of the same ^{99m}Tc and ^{64}Cu half life is negligible in view of the small contribution of these half-lives to the combined uncertainty of the comparison results.

The K4 comparison results are given in Table 5a as well as the linked results A_e in the corresponding BIPM.RI(II)-K1 comparisons which were obtained by multiplying A_E by the linking factors given in Table 5b:

Table 5a: BIPM.RI(II)-K4. comparison results and link to the BIPM.RI(II)-K1 comparisons

Radionuclide	**Measurement method** ACRONYM*	**Solution volume in the ampoules (calculated) /cm^3**	**A_E /kBq**	**$u(A_E)$ /kBq**	**Linked A_e /kBq**	**$u(A_e)$ /kBq**
^{18}F	IC calibrated in June 2017 by 4π(LS)β$^+$-(NaI)γ coincidence 4P-IC-GR-00-00-00 4P-LS-PO-NA-GR-CO	3.606(7), 3.580(7)	10.255	0.041	15 332	64
^{64}Cu	IC calibrated in February 2018 by 4π(LS)β-(NaI)γ coincidence 4P-IC-GR-00-00-00 4P-LS-MX-NA-GR-CO	3.54(2), 3.63(2), 3.55(2)	54.79	0.77	81 200	1100
^{99m}Tc	IC calibrated in October 2018 by 4π(LS)ce-(NaI)γ coincidence 4P-IC-GR-00-00-00 4P-LS-CE-NA-GR-CO	3.621(7), 3.590(7)	12.62	0.11	153 500	1400

* See appendix 1

Table 5b: Linking factors of BIPM.RI(II)-K4 comparison to BIPM.RI(II)-K1 comparison

Radionuclide	**Linking factor**	**Provider of solution for measurement of linking factor at the BIPM**
^{99m}Tc	12 165(23)	LNE-LNHB (2007 and 2014), NPL (2008)
^{18}F	1495.1(18)	LNE-LNHB (2014), AAA* (2014)
^{64}Cu	1482.2(25)	NPL (2016), CNRS/CEMHTI (2015)

* Advanced Accelerator Applications

7. **Key comparison reference values and degrees of equivalence**

7.1 KCRVs update

In May 2013 the CCRI(II) decided to calculate the key comparison reference value (KCRV) using the power-moderated weighted mean [24] rather than an unweighted mean, as had been the policy. This type of weighted mean is similar to a Mandel-Paule mean in that the NMIs' uncertainties may be increased until the reduced chi-squared value is one. In addition, it allows for a power smaller than two in the weighting factor. As proposed in [21], α is taken as $2 - 3/N$ where N is the number of results selected for the KCRV. Therefore, all SIR key comparison results can be selected for the key comparison reference value (KCRV) with the following provisions:

a) only results for solutions standardized by primary techniques are accepted, with the exception of radioactive gas standards (for which results from transfer instrument measurements that are directly traceable to a primary measurement in the laboratory may be included);
b) each NMI or other laboratory has only one result (normally the most recent result or the mean if more than one ampoule is submitted);
c) results more than 20 years old are included in the calculation of the KCRV (but are not included in data shown in the KCDB or in the plots in this report as they have expired);
d) possible outliers can be identified on a mathematical basis and excluded from the KCRV using the normalized error test with a test value of 2.5 and using the modified uncertainties;
e) results can also be excluded for technical reasons; and
f) the CCRI(II) is always the final arbiter regarding excluding any data from the calculation of the KCRV.

All the submissions to the SIR since its inception in 1976 are maintained in a database known as the "master-file". The data set used for the evaluation of the KCRVs is known as the "KCRV file" and is a reduced data set from the SIR master-file.

Although the KCRV may be modified when other NMIs participate, on the advice of the Key Comparison Working Group of the CCRI(II), such modifications are made only by the CCRI(II) during one of its biennial meetings, or by consensus through electronic means (e.g., email) as discussed at the CCRI(II) meeting in 2013. In March 2015 and June 2017, the CCRI agreed for ^{99m}Tc and ^{18}F, respectively, that SIRTI linked results based on primary measurements or pressurized ionization chamber (IC) measurement are eligible for inclusion in the KCRV of the

corresponding BIPM.RI(II)-K1 comparison when the IC is calibrated by a primary measurement of the same radionuclide within one year prior to the comparison date. In 2017, the CCRI also agreed that the limit of one year can be extended for practical reasons when the SIRTI comparison covers more than two nuclides at a time.

The ^{99m}Tc SIR and SIRTI results previously included in the KCRV are given in Table 6a together with the present eligible result. Using these results, the KCRV for ^{99m}Tc calculated using the power moderated weighted mean is 153 060(330) kBq, with the power $\alpha = 1.79$. This can be compared successfully with the previous KCRVs of 153 070(460) kBq published in 2004 [28], 153 140(330) kBq in 2005 [29], 153 240(220) kBq in 2010 [27], 153 170(310) kBq in 2016 [22], 153 090(380) kBq in 2022 [31], 153 050(350) kBq in 2023 [32] and with the value of 153 400(410) kBq obtained using the SIRIC [26] efficiency curves of the SIR.

The ^{18}F SIR and SIRTI results previously included in the KCRV are given in Table 6b together with the present eligible result. Using these results, the KCRV for ^{18}F calculated using the power moderated weighted mean is 15 300(18) kBq, with the power $\alpha = 1.75$. This can be compared with previous KCRVs of 15 241(71) kBq and 15 254(43) kBq published in 2003 [18, 19], 15 245(32) kBq in 2004 [16], 15 259(29) kBq in 2006 [25], 15 276(24) kBq published in 2016 [14], 15 293(19) kBq in 2022 [31] and 15 297(18) kBq in 2023 [32].

The KCRV for ^{64}Cu has been defined in the frame of the BIPM.RI(II)-K1.Cu-64 comparison using direct contributions to the SIR, and is equal to 80 990(340) kBq [23].

Table 6a: ^{99m}Tc SIR and SIRTI linked results included in the calculation of the KCRV

NMI	Comparison and year of participation	Measurement method	Comparison result A_e / kBq	Reference
IRA	SIR, 1984	IC* calibrated in1984 by 4π(PC)e_c-γ coincidence, HPGe detector** and 4π(NaI)γ counting	153 770(660)	[22]
PTB	SIR, 2005	IC calibrated in Nov. 2005 by 4π(PC)e_c-x and 4π(PPC)e_c-photon coincidences	152 710(640)	[22]
NPL	SIR, 2005	4π(PC)e_c-γ coincidence	153 310(660)	[22]
LNE-LNHB	SIR, 2007	4π(PC)β-γ anti-coincidence	153 180(790)	[22]
NIST	SIRTI, 2009	IC calibrated by anticoincidence measurements 2 months prior the comparison	152 840(730)	[22]
KRISS	SIRTI, 2010	IC calibrated by 4π(LS)β-γ coincidence measurements 3 months prior the comparison	154 100(1400)	[22]
NIM	SIRTI, 2012	IC calibrated by coincidence measurements 4 months prior the comparison	153 100(1200)	[22]
LNMRI/IRD	SIRTI, 2013	IC calibrated by 4π(LS)β-γ anticoincidence meas. 1 month prior the comparison	154 700(1700)	[22]
IFIN-HH	SIRTI, 2013	coincidence method	150 400(1800)	[22]
ENEA-INMRI	SIRTI, 2014	4π(LS)ec-γ(NaI) coincidence	150 750(770)	[22]
NMISA	SIRTI, 2015	IC calibrated by 4π(LS)β-γ coincidence measurements 2 months prior the comparison	156 100(2200)	[21]
POLATOM	SIRTI, 2016	4π(LS)ce-γ coincidence	154 600(1200)	[31]
NRC	SIRTI, 2017	IC calibrated by 4π(PC)ce-γ coincidence 8 months prior the comparison	152 500(1500)	[32]
ANSTO	SIRTI, 2017	IC calibrated by 4π(LS)-γ anti-coincidence 11 months after the comparison	153 500(1400)	Present publication

* pressurized ionization chamber (IC) with correction factor for self-absorption in the solution of 1.0037(10)

** calibrated using ^{57}Co and ^{139}Ce calibrated sources

Table 6b: ^{18}F SIR and SIRTI linked results included in the calculation of the KCRV

NMI	Comparison and year of participation	Measurement method	Comparison result A_e / kBq	Reference
IRA	SIR, 2001	IC calibrated by 4πγ(NaI) counting and liquid scintillation	15 312(57)	[14]
NPL	SIR, 2003	4π(PC)β$^+$–γ coincidence method	15 281(39)	[14]
CIEMAT	SIR, 2004	IC calibrated by 4πβ$^+$(PPC)-γ coincidence	15 216(97)	[14]
PTB	SIR, 2005	IC calibrated by 4πβ$^+$(PC)-γ coincidence and CIEMAT/NIST	15 316(50)	[14]
LNE-LNHB	SIR, 2010	Liquid scintillation counting using TDCR	15 203(62)	[14]
VNIIM	SIRTI, 2014	4πγ(NaI) counting	15 197(97)	[20]
ENEA-INMRI	SIRTI, 2014	4π(LS)β$^+$–γ coincidence method, 4πγ(NaI) counting, and TDCR	15 368(49)	[20]
NMISA	SIRTI, 2015	IC calibrated by 4π(LS)β$^+$–γ coincidence method 1 month prior the comparison	15 328(96)	[21]
NIST	SIRTI, 2016	IC calibrated by 4π(LS)β$^+$–γ anticoincidence method 9 months prior the comparison	15 291(64)	[15]
POLATOM	SIRTI, 2016	4π(LS)ce-γ coincidence	15 323(88)	[31]
NRC	SIRTI, 2017	IC calibrated by 4π(PC)β$^+$-γ anti-coincidence counting 5 months prior the comparison	15 332(56)	[32]
ANSTO	SIRTI, 2017	IC calibrated by 4π(LS)β$^+$-γ coincidence 5 months prior the comparison	15 332(64)	Present publication

7.2 Degrees of equivalence

Every participant in a key comparison is entitled to have one result included in the key comparison database (KCDB) as long as the laboratory is a signatory or designated institute listed in the CIPM MRA. Normally, the most recent result is the one included. Any participant may withdraw its result only if all the participants agree.

The degree of equivalence of a particular NMI, i, with the KCRV is expressed as the difference D_i with respect to the KCRV

$$D_i = A_{ei} - \text{KCRV} \quad (1)$$

and the expanded uncertainty ($k = 2$) of this difference, U_i, known as the equivalence uncertainty, hence

$$U_i = 2u(D_i), \quad (2)$$

taking correlations into account as appropriate [24].

The degree of equivalence between any pair of NMIs, i and j, is expressed as the difference D_{ij} in their results

$$D_{ij} = D_i - D_j = A_{ei} - A_{ej} \quad (3)$$

and the expanded uncertainty of this difference U_{ij} where

$$U_{ij}^2 = 4u^2(D_{ij}) = 4\left[u_i^2 + u_j^2 - 2u(A_{ei}, A_{ej})\right] \quad (4)$$

where any obvious correlations between the NMIs (such as a traceable calibration) are subtracted using the covariance $u(A_{ei}, A_{ej})$, as is the correlation coming from the link of the SIRTI to the SIR. The covariance between two participants in the K4 comparison is given by

$$u(A_{ei}, A_{ej}) = A_{ei} A_{ej} (u_L/L)^2 \quad (5)$$

where u_L is the standard uncertainty of the linking factor L given above. However, the CCRI decided in 2011 that these pair-wise degrees of equivalence no longer need to be published as long as the methodology is explained.

Tables 7(a,b,c) show the matrices of the degrees of equivalence with the KCRV as they will appear in the KCDB. It should be noted that for consistency within the KCDB, a simplified level of nomenclature is used with A_{ei} replaced by x_i. The introductory text is that agreed for the comparison. The graph of the degrees of equivalence with respect to the KCRV (identified as x_R in the KCDB) is shown in Figure 3(a,b,c) in relative terms. The graphical representation indicates in part the degree of equivalence between the NMIs but obviously does not take into account the correlations between the different NMIs.

The degrees of equivalence of the BIPM.RI(II)-K1 key comparisons for ^{99m}Tc and ^{18}F have been updated following the update of the KCRV for ^{99m}Tc and ^{18}F.

Conclusion

In 2017, the ANSTO (Australia) hosted the SIRTI to participate in the BIPM ongoing key comparison for activity measurement of ^{18}F, ^{64}Cu and ^{99m}Tc (the BIPM.RI(II)-K4 series). These K4 comparisons are linked to the corresponding BIPM.RI(II)-K1 comparisons (the SIR comparisons).

The key comparison reference values for ^{99m}Tc and ^{18}F, usually defined in the frame of the K1 comparisons, have been updated to include the ANSTO result from the K4 comparisons. The degrees of equivalence with the respective key comparison reference values have been evaluated for ANSTO's participation in the BIPM.RI(II)-K4 comparisons, and degrees of

equivalence for other K1 or K4 participants have been updated. The degrees of equivalence have been approved by the CCRI(II) and are published in the BIPM key comparison database.

Other results may be added when other NMIs contribute with ^{18}F, ^{64}Cu and ^{99m}Tc activity measurements to the K4 or K1 comparisons or take part in other linked Regional Metrology Organization comparisons. It should be noted that the final data in this paper, while correct at the time of publication, will become out-of-date as NMIs make new comparisons. The formal results under the CIPM MRA [7] are those available in the KCDB.

Table 7a. Table of degrees of equivalence and introductory text for ^{99m}Tc

Key comparison BIPM.RI(II)-K1.Tc-99m

MEASURAND : Equivalent activity of ^{99m}Tc

Key comparison reference value: the SIR reference value for this radionuclide is x_R = 153.06 MBq with a standard uncertainty, u_R = 0.33 MBq (see Final Report).
The value x_i is the equivalent activity for laboratory *i*.

The degree of equivalence of each laboratory with respect to the reference value is given by a pair of terms: $D_i = (x_i - x_R)$ and U_i, its expanded uncertainty (k = 2), both expressed in MBq, and $U_i = 2((1 - 2w_i)u_i^2 + u_R^2)^{1/2}$ where w_i is the weight of laboratory *i* contributing to the calculation of x_R.

Linking BIPM.RI(II)-K4.Tc-99m to BIPM.RI(II)-K1.Tc-99m

The value x_i is the SIRTI equivalent activity for laboratory *i* participant in BIPM.RI(II)-K4.Tc-99m having been normalized using the NPL and the LNE-LNHB as linking laboratories (see Final report).
The degree of equivalence of laboratory *i* participant in BIPM.RI(II)-K4.Tc-99m with respect to the key comparison reference value is given by a pair of terms: $D_i = (x_i - x_R)$ and U_i, its expanded uncertainty (k = 2), both expressed in MBq, $U_i = 2((1 - 2w_i)u_i^2 + u_R^2)^{1/2}$ where w_i is the weight of laboratory *i* contributing to the calculation of x_R.

These statements make it possible to extend the BIPM.RI(II)-K1.Tc-99m matrices of equivalence to the other participants in BIPM.RI(II)-K4.Tc-99m.

Table 7a continued

Lab *i* ⇩	D_i / MBq	U_i / MBq
PTB	-0.4	1.3
LNE-LNHB	0.1	1.6
NPL	0.2	1.6
NIST	-0.2	1.4
KRISS	1.0	2.7
NMIJ	-0.7	2.3
NIM	0.0	2.4
CNEA	7.1	4.3
LNMRI/IRD	1.6	3.3
IFIN-HH	-2.2	2.9
VNIIM	3.5	4.8
ENEA-INMRI	-2.3	1.5
NMISA	3.0	4.3
POLATOM	1.5	2.4
NRC	-0.6	2.9
ANSTO	0.4	2.7

Figure 3a. Graph of degrees of equivalence with the KCRV for ^{99m}Tc
(as it appears in Appendix B of the MRA)

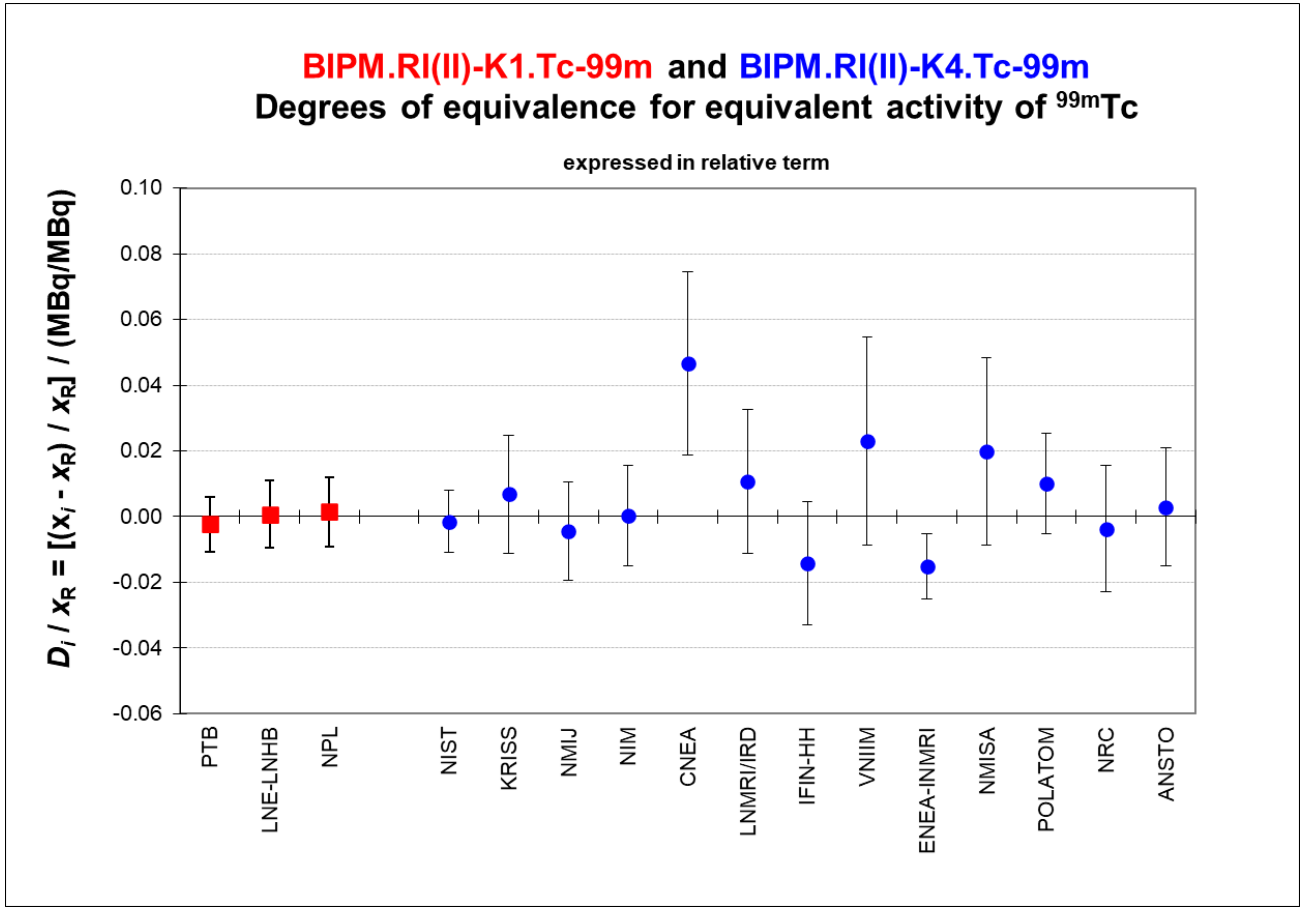

Table 7b. Introductory text and table of degrees of equivalence for ^{18}F

Key comparison BIPM.RI(II)-K1.F-18

MEASURAND : Equivalent activity of ^{18}F

Key comparison reference value: the SIR reference value for this radionuclide is x_R = 15 300 kBq with a standard uncertainty, u_R = 18 kBq (see Final Report). The value x_i is the equivalent activity for laboratory *i*.

The degree of equivalence of each laboratory with respect to the reference value is given by a pair of terms: $D_i = (x_i - x_R)$ and U_i, its expanded uncertainty (k = 2), both expressed in MBq, and $U_i = 2((1 - 2w_i)u_i^2 + u_R^2)^{1/2}$ when each laboratory has contributed to the calculation of x_R.

Linking BIPM.RI(II)-K4.F-18 to BIPM.RI(II)-K1.F-18

The value x_i is the SIRTI equivalent activity for laboratory *i* participant in BIPM.RI(II)-K4.F-18 multiplied by the linking factor to BIPM.RI(II)-K1.F-18 (see Final Report).

The degree of equivalence of laboratory *i* participant in BIPM.RI(II)-K4.F-18 with respect to the key comparison reference value is given by a pair of terms: $D_i = (x_i - x_R)$ and U_i, its expanded uncertainty (k = 2), both expressed in MBq. The approximation $U_i = 2(u_i^2 + u_R^2)^{1/2}$ is used in the following table.

These statements make it possible to extend the BIPM.RI(II)-K1.F-18 matrices of equivalence to all participants in the BIPM.RI(II)-K4.F-18 comparisons.

Table 7b continued

Lab *i* ⇩	D_i / MBq	U_i / MBq
CIEMAT	-0.08	0.19
PTB	0.016	0.094
LNE-LNHB	-0.10	0.12
VNIIM	-0.10	0.19
NPL	0.01	0.11
ENEA-INMRI	0.068	0.092
NMISA	0.03	0.19
NIST	-0.01	0.12
POLATOM	0.02	0.17
NRC	0.03	0.11
ANSTO	0.03	0.12

Figure 3b. Graph of degrees of equivalence with the KCRV for ^{18}F
(as it appears in Appendix B of the MRA)

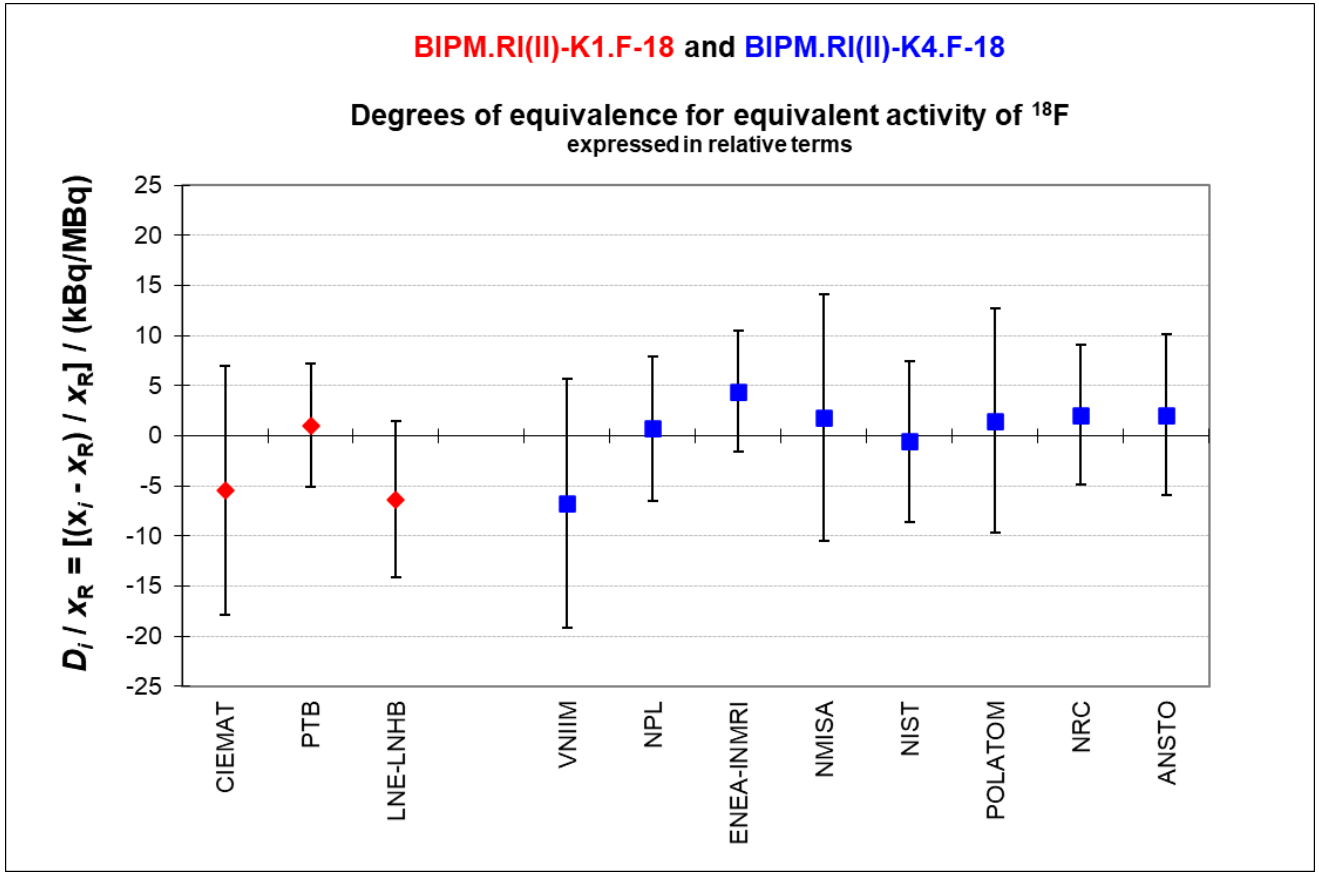

Table 7c. Table of degrees of equivalence and introductory text for ^{64}Cu

Key comparison BIPM.RI(II)-K1.Cu-64

MEASURAND : Equivalent activity of ^{64}Cu

Key comparison reference value: the SIR reference value x_R for this radionuclide is 80.99 MBq, with a standard uncertainty u_R of 0.34 MBq.
The value x_i is taken as the equivalent activity for laboratory i.

The degree of equivalence of each laboratory with respect to the reference value is given by a pair of terms: $D_i = (x_i - x_R)$ and U_i, its expanded uncertainty ($k = 2$), both expressed in MBq, and $U_i = 2((1 - 2w_i)u_i^2 + u_R^2)^{1/2}$ when each laboratory has contributed to the calculation of x_R.

Linking BIPM.RI(II)-K4.Cu-64 to BIPM.RI(II)-K1.Cu-64

The value x_i is the SIRTI equivalent activity for laboratory i participant in BIPM.RI(II)-K4.Cu-64 multiplied by the linking factor to BIPM.RI(II)-K1.Cu-64 (see Final Report).

The degree of equivalence of laboratory i participant in BIPM.RI(II)-K4.Cu-64 with respect to the key comparison reference value is given by a pair of terms: $D_i = (x_i - x_R)$ and U_i, its expanded uncertainty ($k = 2$), both expressed in MBq.
The approximation $U_i = 2(u_i^2 + u_R^2)^{1/2}$ is used in the following table.

These statements make it possible to extend the BIPM.RI(II)-K1.Cu-64 matrices of equivalence to all participants in the BIPM.RI(II)-K4.Cu-64 comparisons.

Lab i ⇩

	D_i / MBq	U_i / MBq
PTB	**0.41**	0.80
CMI-IIR	**-1.2**	1.4
NPL	**0.0**	1.0
LNE-LNHB	**0.3**	1.2
ENEA-INMRI	**-0.2**	1.4

Table 7c continued

	D_i / MBq	U_i / MBq
NIST	-0.4	1.2
POLATOM	0.6	1.2
NRC	0.9	2.3
ANSTO	0.2	2.3

Figure 3c. Graph of degrees of equivalence with the KCRV for ^{64}Cu
(as it appears in Appendix B of the MRA)

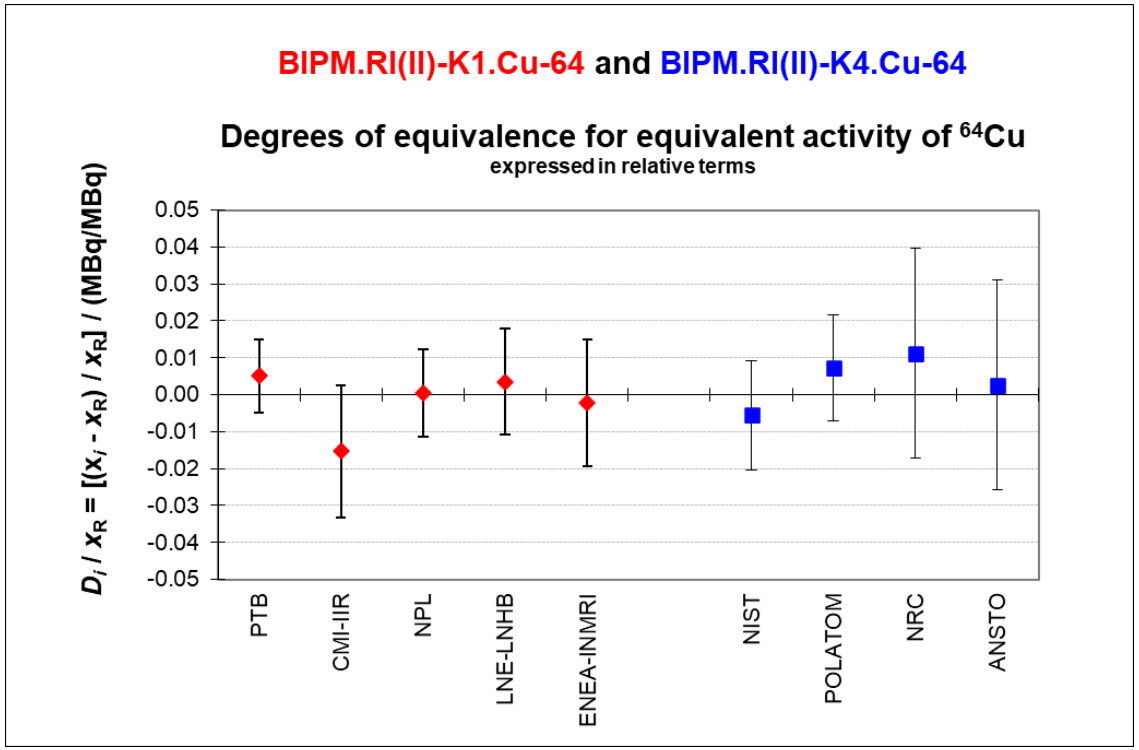

References

[1] Ratel G., The Système International de Référence and its application in key comparisons, *Metrologia*, 2007, **44**(4), S7-S16.

[2] Remit of the CCRI(II) Transfer Instrument Working Group, 2009, CCRI(II) working document CCRI(II)/09-15.

[3] Bé M.-M., Chisté V., Dulieu C., Browne E., Chechev V., Kuzmenko N., Helmer R., Nichols A., Schönfeld E., Dersch R., Table of radionuclides, 2004, *Monographie BIPM*-5, volume 1.

[4] Bé M.-M., Helmer R., 2011, Decay Data Evaluation Project working group, www.nucleide.org/ DDEP_WG/DDEPdata.htm.

[5] NUDAT2.5, National Nuclear Data Center, Brookhaven National Laboratory, based on ENSDF and the Nuclear Wallet Cards.

[6] Bouchard J., MTR2: a discriminator and dead-time module used in counting systems, *Appl. Radiat. Isot.*, 2000, **52**, 441-446.

[7] SIR Transfer Instrument. Protocol for the ongoing comparisons on site at the NMIs, BIPM.RI(II)-K4. Published on the CIPM MRA KCDB website.

[8] CIPM MRA: *Mutual recognition of national measurement standards and of calibration and measurement certificates issued by national metrology institutes*, International Committee for Weights and Measures, 1999, 45 pp. http://www.bipm.org/pdf/mra.pdf.

[9] Michotte C. *et al*., The SIRTI, a new tool developed at the BIPM for comparing activity measurements of short-lived radionuclides world-wide, *Rapport BIPM*-2013/02.

[10] Michotte C. *et al*., Calibration of the SIRTI against the SIR and trial comparison of ^{18}F and ^{99m}Tc at the NPL. *In preparation*.

[11] Baerg A.P. *et al.*, Live-timed anti-coincidence counting with extending dead-time circuitry, *Metrologia*, 1976, **12**, 77-80.

[12] Fitzgerald R., Corrections for the combined effects of decay and dead time in live-timed counting of short-lived radionuclides, *Appl. Radiat. Isot.*, 2016, **109**, 335-340.

[13] Sibbens G., A comparison of NIST/SIR-, NPL-, and CBNM 5 ml ampoules, 1991, GE/R/RN/14/91, CEC-JRC Central Bureau for Nuclear Measurements, Belgium.

[14] Michotte C. et al., Update of the BIPM comparison BIPM.RI(II)-K1.F-18 of activity measurements of the radionuclide ^{18}F to include the 2010 result of the LNE-LNHB (France). *Metrologia*, 2016, **53,** *Tech. Suppl.*, 06004.

[15] Michotte C., Nonis M., Bergeron D., Cessna J., Fitzgerald R., Pibida L., Zimmerman B., Fenwick A., Ferreira K., Keightley J., Da Silva I., Activity measurements of the radionuclides ^{18}F and ^{64}Cu for the NIST, USA, in the ongoing comparisons BIPM.RI(II)-K4.F-18 and BIPM.RI(II)-K4.Cu-64, *Metrologia*, 2017, **54**, Tech. Suppl. 06011.

[16] Ratel G., Michotte C., García-Toraño E., Los Arcos J.-M., Update of the BIPM comparison BIPM.RI(II)-K1.F-18 of activity measurements of the radionuclide ^{18}F to include the CIEMAT, *Metrologia*, 2004, **41**, *Tech. Suppl.*, 06016.

[17] Ratel G., Michotte C., Woods M.J., Comparisons CCRI(II)-K3.F-18 and APMP.RI(II)-K3.F-18 of activity measurements of the radionuclide ^{18}F and links to the key comparison reference value of the BIPM.RI(II)-K1.F-18 comparison, *Metrologia*, 2005, **42**, *Tech. Suppl.*, 06007.

[18] Ratel G., Michotte C., BIPM comparison BIPM.RI(II)-K1.F-18 of activity measurements of the radionuclide ^{18}F, *Metrologia*, 2003, **40**, *Tech. Suppl.*, 06005.

[19] Ratel G., Michotte C., Woods M.J., Update of the BIPM comparison BIPM.RI(II)-K1.F-18 of activity measurements of the radionuclide ^{18}F to include the NPL, *Metrologia*, 2003, **40**, *Tech. Suppl.*, 06027.

[20] Michotte C., Nonis M., Alekseev I.V., Kharitonov I.A., Tereshchenko E.E., Zanevskiy A.V., Keightley J.D., Fenwick A., Ferreira K., Johansson L., Capogni M., Carconi P., Fazio A., De Felice P., Comparison of ^{18}F activity measurements at the VNIIM, NPL and the ENEA-INMRI using the SIRTI of the BIPM, *Applied Radiation and Isotopes*, 2016, **109**, 17–23.
[21] Michotte C., Nonis M., Van Rooy M.W., Van Staden M.J. and Lubbe J., Activity measurements of the radionuclides ^{18}F and ^{99m}Tc for the NMISA, South Africa in the ongoing comparisons BIPM.RI(II)-K4.F-18 and BIPM.RI(II)-K4.Tc-99m, *Metrologia*, 2017, **54**, *Tech. Suppl.*, 06001.
[22] Michotte C., Nonis M., Alekseev I.V., Kharitonov I.A., Tereshchenko E.E., Zanevskiy A.V., Capogni M., De Felice P., Fazio A., Carconi P., Activity measurements of the radionuclide ^{99m}Tc for the VNIIM, Russian Federation and ENEA-INMRI, Italy, in the ongoing comparison BIPM.RI(II)-K4.Tc-99m and KCRV update in the BIPM.RI(II)-K1.Tc-99m comparison, *Metrologia*, 2016, **53**, *Tech.Suppl.*, 06014.
[23] Michotte C., *et al*., Update of the BIPM comparison BIPM.RI(II)-K1.Cu-64 of activity measurements of the radionuclide ^{64}Cu to include the 2009 results of the CMI–IIR (Czech Rep.) and the NPL (UK), the 2010 result of the LNE–LNHB (France) and the 2011 result of the ENEA–INMRI (Italy), *Metrologia*, 2013, **50**, *Tech. Suppl.*, 06021.
[24] Pommé S., Keightley, J., Determination of a reference value and its uncertainty through a power-moderated mean, *Metrologia*, 2015, 52(3), S200-S212.
[25] Ratel G., Michotte C., Kossert K., Janßen H., Update of the BIPM comparison BIPM.RI(II)-K1.F-18 of activity measurements of the radionuclide ^{18}F to include the PTB, *Metrologia*, 2006, **43**, *Tech. Suppl.*, 06001.
[26] Cox M.G., Michotte C., Pearce A.K., Measurement modelling of the International Reference System (SIR) for gamma-emitting radionuclides, Monographie BIPM-7, 2007, 48 pp.
[27] Michotte C., Courte S., Ratel G., Moune M., Johansson L., Keightley J., Update of the BIPM.RI(II)-K1.Tc-99m comparison of activity measurements for the radionuclide ^{99m}Tc to include new results for the LNE-LNHB and the NPL, *Metrologia*, 2010, **47**, *Tech. Suppl*., 06026.
[28] Ratel G., Michotte C., BIPM comparison BIPM.RI(II)-K1.Tc-99m of activity measurements of the radionuclide ^{99m}Tc, *Metrologia*, 2004, **41**, *Tech. Suppl*., 06005.
[29] Ratel G., Michotte C., Johansson L., Update of the BIPM.RI(II)-K1.Tc-99m comparison of activity measurements for the radionuclide ^{99m}Tc to include the NPL, *Metrologia*, 2005, **42**, *Tech. Suppl*., 06015.
[30] Galea R., Michotte C., Nonis M., Moore K., El Gamal I., Keightley J., Fenwick A., *Applied Radiation and Isotopes*, 2019, **154,** 108834.
[31] Michotte C., Dziel T., Listkowska A., Ziemek T., Tymiński Z. and Da Silva I., Activity measurements of the radionuclides ^{99m}Tc, ^{18}F and ^{64}Cu for the POLATOM, Poland, in the ongoing comparisons BIPM.RI(II)-K4 series and KCRV update in the corresponding BIPM.RI(II)-K1 comparison, *Metrologia*, 2022, **59**, *Tech. Suppl*., 06004.
[32] Michotte C., Nonis M., Galea R., Moore K., El Gamal I. El., Da Silva I., Activity measurements of the radionuclides ^{18}F, ^{64}Cu, ^{99m}Tc and ^{11}C for the NRC, Canada, in the ongoing comparisons BIPM.RI(II)-K4 series and KCRV update in the corresponding BIPM.RI(II)-K1 comparison, *Metrologia*, 2023, **60**, Tech. Suppl., 06006.
[33] Funck and Nylandstedt Larsen, *Int. J. Appl. Radiat, Isot.*, 1983, **34,** 565.
[34] van Wyngaardt W.M. *et al*., Primary standardisation of technetium-99m by liquid scintillation coincidence counting, *Appl. Radiat. Isot.*, 2020, **156**, 108935.

Appendix 1. **Acronyms used to identify different measurement methods**
Each acronym has six components, geometry-detector (1)-radiation (1)-detector (2)-radiation (2)-mode. When a component is unknown, ?? is used and when it is not applicable, 00 is used.

Geometry	**acronym**	**Detector**	**acronym**
4π	4P	proportional counter	PC
defined solid angle	SA	press. prop. counter	PP
2π	2P	liquid scintillation counting	LS
undefined solid angle	UA	NaI(Tl)	NA
		Ge(HP)	GH
		Si(Li)	SL
		CsI(Tl)	CS
		ionization chamber	IC
		grid ionization chamber	GC
		Cerenkov detector	CD
		calorimeter	CA
		solid plastic scintillator	SP
		PIPS detector	PS
		CeBr3	CB
Radiation	**acronym**	**Mode**	**acronym**
positron	PO	efficiency tracing	ET
beta particle	BP	internal gas counting	IG
Auger electron	AE	CIEMAT/NIST	CN
conversion electron	CE	sum counting	SC
mixed electrons	ME	coincidence	CO
bremsstrahlung	BS	anti-coincidence	AC
gamma rays	GR	coincidence counting with efficiency tracing	CT
X - rays	XR	anti-coincidence counting with efficiency tracing	AT
photons (x + γ)	PH	triple-to-double coincidence ratio counting	TD
alpha - particle	AP	selective sampling	SS
mixture of various radiations	MX	high efficiency	HE

Examples

Method	**acronym**
4π(PC)β–γ-coincidence counting	4P-PC-BP-NA-GR-CO
4π(PPC)β–γ-coincidence counting eff. trac.	4P-PP-MX-NA-GR-CT
defined solid angle α-particle counting with a PIPS detector	SA-PS-AP-00-00-00
4π(PPC)AX-γ(Ge(HP))-anticoincidence counting	4P-PP-MX-GH-GR-AC
4π CsI-β,AX,γ counting	4P-CS-MX-00-00-HE
calibrated IC	4P-IC-GR-00-00-00
internal gas counting	4P-PC-BP-00-00-IG

Appendix 2a. Uncertainty budget for the IC calibration done by ^{18}F 4P-LS-PO-NA-GR-CO primary measurements (June 2017).

Uncertainty Contributions due to	**Comments**	**Evaluation method**	**Relative standard uncertainties x10^4**
Counting statistics (for primary determination)	Standard deviation of four results from 2 sources (double- and triple-coincidence counts for LS channel)	A	**4**
Decay data	From uncertainty in DDEP β^+/EC branching ratio = 0.9686 (19)	B	**20**
Dead time	Effect of dead time on results assessed by varying τ_D = (50 ± 10) μs	B	**1**
Resolving time	Effect of resolving time on results assessed by varying τ_R = 100 (+ 100 ns)	B	**7**
Extrapolation	Maximum difference between B vs C/G and BG/C vs (G/C-1), linear and cubic polynomials	B	**15**
Background (primary)	Variation of background according to counting statistics	A	**5**
Weighing	Weighing, dilution and solution handling	B	**20**
Decay correction	From uncertainty of DDEP half life = 1.82890 (23) hrs, max decay correction > 12 half-lives	B	**11**
Counting statistics (IC response determination)	Standard deviation of the mean for 50 sets of 100 measurements	A	**1**
Impurities	None detected		**-**
Relative combined standard uncertainty			**36**

Appendix 2b. Uncertainty budget for the IC calibration done by ^{64}Cu 4P-LS-MX-NA-GR-CO primary measurements (February 2018).

Uncertainty Contributions due to	**Comments**	**Evaluation method**	**Relative standard uncertainties x10^4**
Counting statistics (for primary determination)	Standard deviation of the mean for 3 sources	A	**75**
Decay data	Uncertainty in correction for different detection probabilities for $ec_{0,0}$ and $ec_{1,0}$ branches	B	**21**
Dead time	Effect of dead time on results assessed by varying τ_D = (50 ± 10) μs	B	**25**
Resolving time	Effect of resolving time on results assessed by varying τ_R = (200 ± 50) ns	B	**3**
Extrapolation	Difference between weighted and unweighted fits, and variation observed when removing high-efficiency data points	B	**100**
Background (primary)	Gamma background rate = (4.11 ± 0.04) s^{-1}	B	**52**
Weighing	Weighing, dilution and solution handling	B	**10**
^{64}Cu half life	From uncertainty of DDEP half life = 12.7004 (20) hrs	B	**6**
Counting statistics (IC response determination)	Standard deviation of the mean for 50 sets of 100 measurements	A	**1**
Impurities	None detected		**-**
Relative combined standard uncertainty			**140**

Appendix 2c. Uncertainty budget for the IC calibration done by ^{99m}Tc 4P-LS-CE-NA-GR-CO primary measurements (October 2018).

Uncertainty Contributions due to	**Comments**	**Evaluation method**	**Relative standard uncertainties x10^4**
Counting statistics (for primary determination)	Theoretical standard deviation of the weighted mean for 5 sources	A	12
Decay data	Uncertainty in correction for non-detection of $\gamma_{2,0}$ transition	B	1.4
Dead time	Effect of dead time on results assessed by varying τ_D = (50 ± 10) μs	B	6
Resolving time	Effect of resolving time on results assessed by varying τ_R = (200 ± 100) ns	B	47
Extrapolation	Maximum difference between linear and quadratic polynomial fits	B	65
Weighing	Weighing, dilution and solution handling	B	10
^{99m}Tc half life	From uncertainty of DDEP half life = 6.0067 (10) hrs, LS sources measured over 8.5 half-lives	B	5.8
Counting statistics (IC response determination)	Standard deviation of the mean for 50 sets of 100 measurements	A	1
Measurement method		B	1
Background	Included in counting statistics for measurement variability	A	-
Impurities	None detected		-
Relative combined standard uncertainty			**83**